Periodic Near-field Enhancement on Metal-Dielectric Interfacial Gratings at Optimized Azimuthal Orientation

M. Csete[*1,2], X. Hu[1], Á. Sipos[2], A. Szalai[2], A. Mathesz[2] and K. Berggren[1]
[1]Massachusetts Institute of Technology, Research Laboratory of Electronics, Nanostructures Laboratory,
[2]University of Szeged, Department of Optics and Quantum Electronics
*Corresponding author: MIT RLE NSL, 77 Massachusetts Avenue, MA-02139, mcsete@mit.edu

Abstract: The effect of plasmon-wavelength scaled gratings on the surface plasmon resonance is studied experimentally and theoretically. The model samples are multi-layers containing laser-fabricated gratings at bimetal-polymer interfaces. Dual-angle dependent surface plasmon resonance measurements are performed illuminating the samples by monochromatic light in Kretschmann arrangement. The double-peaked resonance curves show that it is possible to maximize the grating-coupling efficiency by the appropriate azimuthal orientation of the grooves. The dual-angle dependent reflection problem on three dimensional periodic structures is solved by RF module of COMSOL. The numerical calculations prove that the grating-coupling phenomenon is accompanied by periodic near-field enhancement at the metal-dielectric interfaces. The air- and glass-side plasmons are synchronized along the valleys at the optimal azimuthal orientation. The synchronization possibility of the periodic plasmon-field and adhesion enhancement is an important tool to improve the sensitivity in bio-sensing based on the monitoring of the secondary peaks appeared due to rotated grating-coupling phenomenon.

Keywords: surface plasmon resonance, rotated grating-coupling, polar and azimuthal orientation, periodic near-field enhancement

1. Introduction

The presence of periodic structures at metal-dielectric interfaces strongly influence the resonance characteristic of the Surface Plasmon Polaritons. The appearance of photonic energy gaps is accompanied by periodic electromagnetic field and surface charge distributions [1].

Our previous far-field Surface Plasmon Resonance measurements performed on sub-micrometer metal-dielectric interfacial structures have shown that the Rotated Grating-Coupling phenomenon results in double-peaked angle-dependent resonance curves [2].

The conditions of highly efficient coupling are the commensurability of the periodicity with the plasmon wavelength, the appropriately large modulation depth, and the right azimuthal orientation of the grating grooves with respect to the plane of the exciting light incidence.

The complementary Pulsed Force Mode Atomic Force Microscopy measurements performed on laser-generated gratings have shown the coexistence of periodic adhesion modulation. The rotated grating-coupling phenomenon was utilized in bio-sensing of proteins adhered into the highly adhesive grating valleys [3]. The purpose of the COMSOL calculations was to determine the near-field distribution accompanying the detected far-field phenomena, and to explain the experienced enhanced RGC SPR detection sensitivity.

2. Experimental results

The model-samples in present calculations were NBK7 substrates coated by bimetal layers (38 nm silver and 7 nm gold) and covered by a polymer grating having a periodicity of Λ=416 nm and a modulation depth of 2a=33.8 nm.

The gratings were prepared by laser-based Interference Lithography in experimental studies. The fourth harmonic of a Nd:YAG laser (λ_{IL}=266 nm. τ=10 ns) illuminated a master grating, and the first order diffracted beams were recombined at the sample surface resulting in periodic intensity distribution.

The multilayer composition and experimental parameters were set in order to maximize the rotated grating-coupling efficiency [3].

2.1 Topography of laser-fabricated gratings

Tapping Mode Atomic Force Microscopy was applied to map the topography of the laser generated gratings. It was shown that the line-cross-section of the gratings is sinusoidal, according to the intensity distribution of the interference pattern (**Figure 1**).

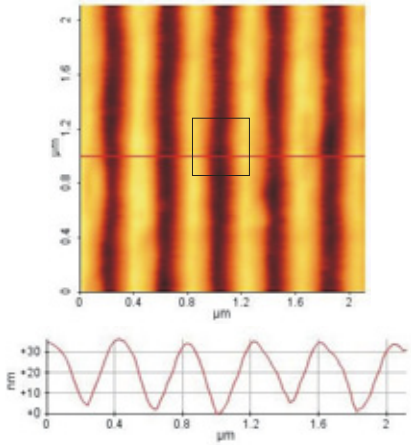

Figure 1. Topography of a grating generated by Nd:YAG laser , applying N=900 pulses having a fluence of F=10.5 mJ/cm^2. The line-cross-section of the gratings is sinusoidal. The inset shows the unit cell applied in model calculations.

2.2 Surface Plasmon Resonance in presence of laser-fabricated gratings

Polar and azimuthal angle dependent SPR measurements were performed in a modified Kretschmann arrangement [2]. The samples were illuminated by monochromatic light having a wavelength of λ_{SPR}=532 nm. The φ polar angle scan was performed collecting the angle dependent reflected light by a photodiode. The **γ** azimuthal orientation of the grating grooves with respect to the plane of light incidence was set by rotating the samples with $\Delta\boldsymbol{\gamma} = 15^o$ between measurements.

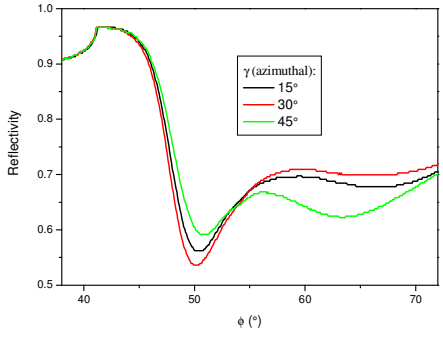

Figure 2. Surface Plasmon Resonance curves measured on multi-layers containing laser fabricated grating at three different azimuthal orientations.

The SPR measurements have shown that secondary peaks are detectable in the entire azimuthal angle interval of $\boldsymbol{\gamma} = 0\text{-}90^o$, but the depth of these minima is considerably larger around the optimal value of $\boldsymbol{\gamma} = 30^o$ (**Figure 2**).

3. Use of COMSOL Multiphysics

The RF COMSOL module was applied, and the "Harmonic wave propagation" was studied in order to determine the EM field distribution in the multi-layer stack. The geometry of the model consisted of one unit cell of the periodic structure (**Figure 3**). Floquet periodic boundary conditions were combined with Port-boundary conditions to describe the periodic nature of the problem, and to specify the illumination by p-polarized light, respectively.

The illumination from the bottom was described in Port boundary condition by specifying the **H** field of the oblique incident plane wave with in plane polarization, taking the φ polar and γ azimuthal angles according to the experiments into account:

$$H_{x\_TM} \cdot \exp(-j(k_x \cdot x + k_y \cdot y)), \text{(1a)}$$

$$H_{y\_TM} \cdot \exp(-j(k_x \cdot x + k_y \cdot y)), \text{(1b)}$$

$$H_{z\_TM} \cdot \exp(-j(k_x \cdot x + k_y \cdot y)), \text{(1c)}$$

where the components of the **H** vector are:

$$H_{x\_TM} = H_0 \cdot \cos\gamma, \text{(2a)}$$

$$H_{y\_TM} = H_0 \cdot \sin\gamma, \text{(2b)}$$

$$H_{z\_TM} = 0, \qquad \text{(2c)}$$

while the components of the **k** wave vector are:

$$k_x = k_0 \cdot \sin\varphi \cdot \sin\gamma, \text{(3a)}$$

$$k_y = k_0 \cdot \sin\varphi \cdot \cos\gamma, \text{(3b)}$$

$$k_z = k_0 \cdot \cos\varphi. \qquad \text{(3c)}$$

The geometry of the model included the following media: NBK7 substrate, bimetal layers consisting of silver and gold, a grating made of polymer (poly-carbonate) and an air-filled closing layer at the top. The indexes of refraction of the NBK7 and polymer dielectric media were specified by Cauchy-formulas determined via ellipsometry. The complex permittivity of the metal layers was specified by combined Drude-Lorentz model fitting the dielectric parameters measured on thin films [4].

The normal density of the applied periodic meshes made possible to meet the Nyquist criterion and to study the field distribution along the polymer stripes (**Figure 3**).

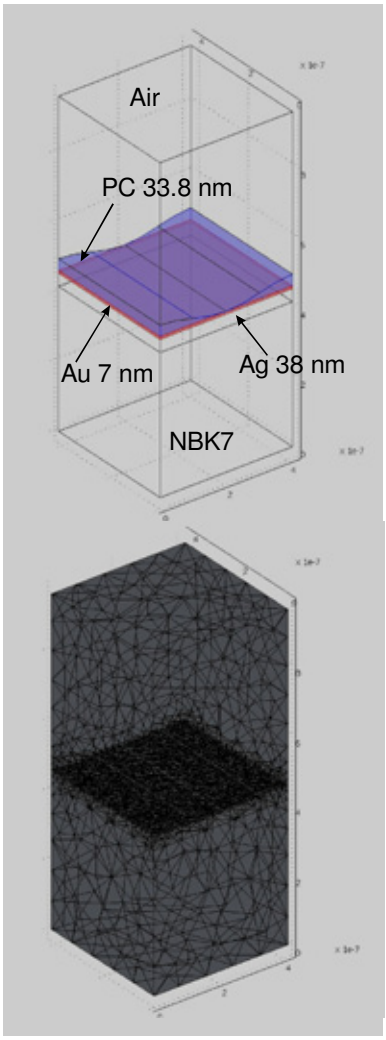

Figure 3. Three dimensional model applied to determine the dual-angle dependent near-field distribution, and the normal density periodic grid.

4. Discussion

The SPR measurements have proven that the $\gamma = 30^{\circ}$ is an optimal azimuthal orientation, where the secondary peak is the deepest. The FEM calculations provided the near-field origin of this phenomenon.

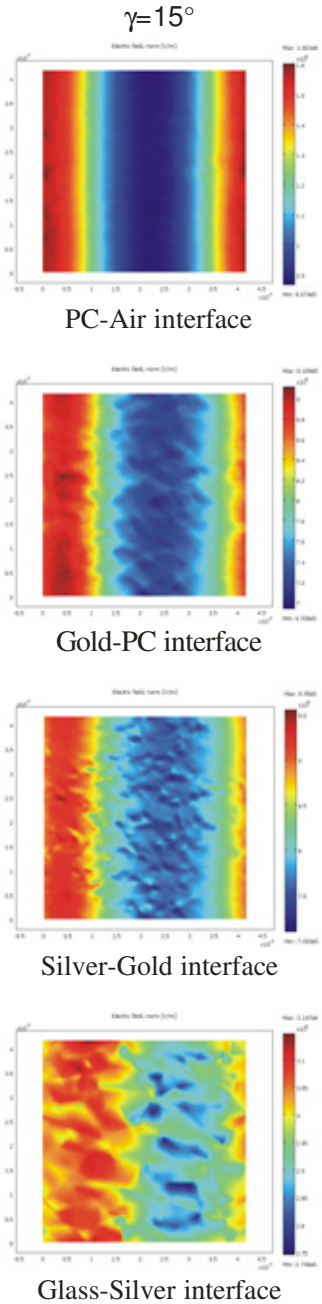

Figure 4. The near-field distribution at different interfaces of the multilayer at $\gamma = 15^{\circ}$ azimuthal orientation. The maxima of the normalized electric field are arrayed along the right side of the polymer stripes.

The polar angle was set to $\varphi = 50.5^{\circ}$ according to the position of the measured secondary minima, and the azimuthal orientation of the grating grooves with respect to the plane of light incidence was varied by $\Delta\gamma = 15^{\circ}$ steps. The local field enhancement was visualized by extracting the normalized electric field at different interfaces.

The model calculations have shown that there is a periodic near-field enhancement parallel to the polymer stripes on both of the opposite metal-dielectric interfaces, due to the coupling on the grating having a periodicity commensurable with the plasmon wavelength.

At the azimuthal orientation of $\gamma = 15^{\circ}$ the normalized electric field maxima are aligned along the polymer stripes, and are right-shifted with respect to the unit cell, i.e. the left side of the valleys is partially illuminated (**Figure 4**). The shift is different for the air- and the glass-side maxima, revealing to plasmon fields which are still de-synchronized spatially.

The peculiarity of the $\gamma = 30^{\circ}$ azimuthal orientation corresponding to the deepest measured plasmon resonance peaks is that the positions of the normalized electric-field maxima are closely synchronized with respect to the unit cell (**Figure 5**). This indicates that the air-side and the glass-side plasmons are excited synchronously along the grating valleys with high efficiency. Taking into account the small layer thicknesses, these plasmon fields may overlap and couple. This is the explanation of the largest depth of the secondary peaks, which indicate the highest coupling efficiency at this particular azimuthal orientation.

At the azimuthal orientation of $\gamma = 45^{\circ}$ the normalized electric field maxima are aligned again closely along the polymer stripes, but they are left-shifted with respect to the unit cell (**Figure 6**). The shift is larger in case of the glass-side plasmons indicating that the glass- and air-side plasmons started to be de-synchronized.

The presence of the grating may result in dual plasmon field at the opposite metal-dielectric interfaces, which can be coupled at the optimal azimuthal orientation with high efficiency. When the EM field maxima are synchronized in the valleys, the near-field is synchronized also with the periodic adhesion modulation, enhancing the sensitivity of RGC SPR bio-sensing.

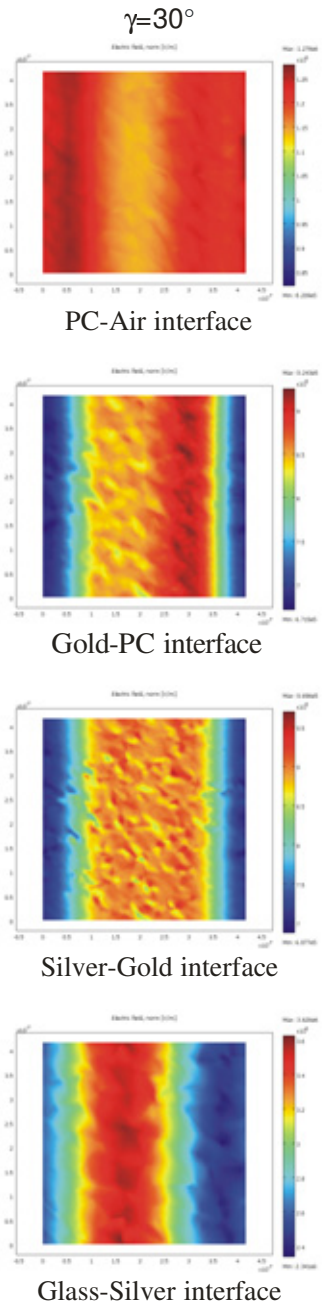

Figure 5. The near-field distribution at different interfaces of the multilayer at $\gamma = 30^{\circ}$ azimuthal orientation. The maxima of the normalized electric field are synchronously aligned along the valleys for both of the glass- and air-side plasmons.

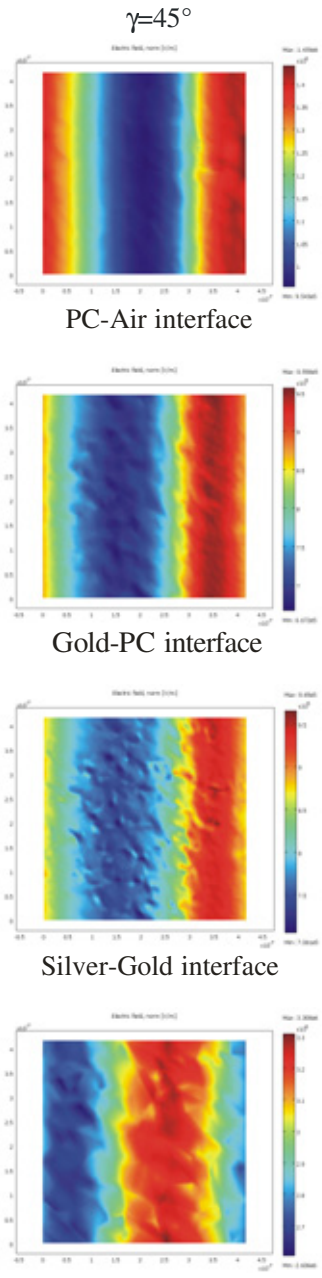

Figure 6. The near-field distribution at different interfaces of the multilayer at $\gamma = 45^{\circ}$ azimuthal orientation. The normalized electric field maxima are arrayed along the right-boundary of the valley on the glass-side, while the air-side plasmon is mostly confined along the PC stripes.

5. Conclusions

The three dimensional COMSOL model calculations have proven that the grating-coupling phenomenon is accompanied by periodic near-field enhancement at both of the metal-dielectric interfaces. The glass-side plasmons are excitable due to the coupling on the grating. At the azimuthal orientation corresponding to the highest coupling efficiency the air- and glass-side plasmons are spatially synchronized along the grating valleys. The advantage of the phenomenon is the collection of the EM-field into the valleys, where the proteins prefer to attach. This is the explanation of the enhanced detection efficiency experienced in our previous bio-sensing studies.

6. References

1. W. L. Barnes, T. W. Preist, S. C. Kitson and J. R. Sambles: Physical origin of photonic energy gaps in the propagation of surface plasmons on gratings, *Phys. Rev. B,* **54/9,** 6227-6244 (1996).
2. M. Csete, A. Kőházi-Kis, V. Megyesi, K. Osvay, Zs. Bor, M. Pietralla, O. Marti: Coupled surface plasmon resonance on bimetallic films covered by sub-micrometer polymer gratings, *Org. Electronics,* **8/2-3,** 148-160 (2007).
3. M. Csete, Á. Sipos, A. Kőházi-Kis, A. Szalai, G. Szekeres, A. Mathesz, T. Csákó, K. Osvay, Zs. Bor, B. Penke, M. A. Deli, Sz. Veszelka, A. Schmatulla, O. Marti: Comparative study of sub-micrometer polymeric structures: dot-arrays, linear and crossed gratings generated by UV laser based two-beam interference, as surfaces for SPR and AFM based bio-sensing, *Appl. Surf. Sci.,* **254/4,** 1194-1205 (2007).
[4] M. A. Ordal, L. L. Long, R. J. Bell, S. E. Bell, R. R. Bell, R. W. Alexander, Jr., and C. A. Ward:Optical properties of the metals Al, Co, Cu, Au, Fe, Pb, Ni, Pd, Pt, Ag, Ti, and W in the infrared and far infrared, *Appl. Opt.,* **22/7,** 1099-1119 (1983).

7. Acknowledgements

Financial support of this research was provided by Hungarian Foundations: OTKA No. CNK 78549 and K 75149. Mária Csete would like to thank the Hungarian Scholarship Board for the Eötvös postdoctoral fellowship.